2021 43rd Annual International Conference of the
IEEE Engineering in Medicine & Biology Society (EMBC)
Oct 31 - Nov 4, 2021. Virtual Conference

Effect of Rotation Sequence on Thoracohumeral Joint Kinematics during Various Shoulder Postures*

Alyssa J. Schnorenberg, and Brooke A. Slavens, *Member, IEEE*

Abstract— **Current methods for selecting a rotation sequence to biomechanically model shoulder joint angles during motion assessment are challenging and controversial due to insufficient knowledge of their effect on the clinical interpretation of movement. Seven rotation sequences were examined by factors including incidences of gimbal lock and joint angle error in two healthy adults during 12 postures using right and left arms. This work was the first to explore the effects of each of the six Cardan angle sequences and the International Society of Biomechanics recommended YXY Euler sequence on the thoracohumeral joint in an array of postures. Results of this work show that there is not a "one size fits all" approach via rotation sequence selection for reliable and coherent expression of shoulder joint postures, particularly of the thoracohumeral joint. For best biomechanical modeling practice, it is recommended that researchers carefully consider the implications of a particular rotation sequence based on the posture or task of interest and resulting incidences of gimbal lock and joint angle error.**

Clinical Relevance— **This work examines the effect of seven different mathematical computations for assessing shoulder joint angles in different postures for application of clinical movement analysis.**

I. Introduction

Upper extremity kinematic analyses can aid both researchers and clinicians in better understanding movement disorders and evaluating the efficacy of rehabilitation strategies. Optical motion capture systems are commonly used in clinical and research applications to capture upper body motion and Cardan-Euler angles are the most frequently used mathematical convention for calculating three-dimensional (3D) joint kinematics [1]. In 2005, the International Society of Biomechanics (ISB) recommended standardized use of the YXY Euler rotation sequence for inverse kinematics modeling of the 3D angles of the glenohumeral and thoracohumeral joints [2, 3]. However, a 2018 review by Valevicius et al. highlighted the dichotomous views in the literature on the ISB recommendations, with less than half of the studies reviewed fully adhering to these guidelines [1]. Those who did not follow the suggested YXY Euler rotation sequence were cited as saying Cardan rotations were 'more clinically relevant, similar to those used in lower limb kinematic analysis…to obtain flexion/extension, abduction/adduction, and axial rotation' [1], as similarly stated by others [4, 5]. While some Cardan sequences appear to be used more commonly than others, all six sequences have been reported in the literature for calculating upper extremity joint kinematics. The inherently large shoulder joint range of motion prevents a singular standard for 3D kinematic analysis [2] as research has shown that no singular sequence is accurate for all motions of the thoracohumeral joint [6]. Another issue is the incidence of gimbal lock, which occurs when the first and third axes of the two coordinate systems are coincident, resulting in an unsolvable rotation sequence [6]. Multiple studies agree the rotation sequence utilized should be based upon the magnitude of the primary shoulder movement of the task, minimal or no incidence of gimbal lock, and the interpretability of the resulting angles [1, 2, 6-8]. However, there are no known studies that have explored the effects of all six cardan sequences and the ISB recommended YXY Euler rotation on the thoracohumeral joint angle calculations during a variety of upper extremity movements. Research is required to provide recommendations for the most accurate rotation sequence to apply for modeling 3D thoracohumeral joint angles. Indeed, it may not be appropriate to use a single rotation sequence when evaluating multiple postures or tasks. This study investigates the effects of multiple rotation sequences on the calculation of thoracohumeral joint angles during static shoulder postures in order to help determine appropriate use.

II. Methods

A. Participants

Two healthy adults participated in this study: one female (age = 27 years, height = 64.5 in, weight = 118 lbs) and one male (age = 33 years, height = 72 in, weight = 210 lbs). Participants were excluded if there was a history or current knowledge of shoulder pain or pathology. The institution's institutional review board approved this study.

B. Experimental Set-up and Procedures

Anthropometric measurements (including: hand thickness at the third metacarpal joint and anterior-posterior elbow thickness) were obtained and passive reflective markers were placed bilaterally on bony anatomical landmarks and technical locations of the participant (Fig. 1). A 15 camera Vicon TS motion analysis system captured the 3D trajectories of the markers at 120 Hz during each task. Each participant performed 12 static poses coinciding with at least one anatomical plane so a goniometer could be used for accurate positioning. Each posture was held for two seconds, for two trials. Postures included: arm abduction of 0° (arms at side), -45°, -90° and -120° within the coronal plane (postures 1-4, respectively), and –30° (extension), 45°, 90°, and 120° (flexion) within the sagittal plane (postures 5-8, respectively).

*Research supported by Marquette University Seeds of Faith Fellowship and NICHD of the NIH award R01HD098698.

A. J. Schnorenberg is with the Department of Biomedical Engineering, Marquette University, Milwaukee, WI 53233 USA and the Department of Rehabilitation Sciences and Technology, University of Wisconsin Milwaukee, Milwaukee, WI 53233 USA (corresponding author: phone: 414-251-7746; e-mail: paulaj@uwm.edu).

B. A. Slavens is with the Department of Rehabilitation Sciences and Technology, University of Wisconsin Milwaukee, Milwaukee, WI 53233 USA (e-mail: slavens@uwm.edu).

The participant was also positioned with their arm adducted to their side and elbow flexed to 90°, thumb pointing superiorly. From this start position the participant's thoracohumeral (TH; humerus relative to thorax) joint was first internally rotated 30° and then externally rotated 30° (postures 9-10, respectively). Lastly, the participant was positioned with their arm abducted 90° in the coronal plane and elbow flexed to 90°, palm facing anteriorly. From this start position the participant's TH joint was first rotated to 30° of internal rotation and then to 90° (parallel with the transverse plane) (postures 11-12, respectively).

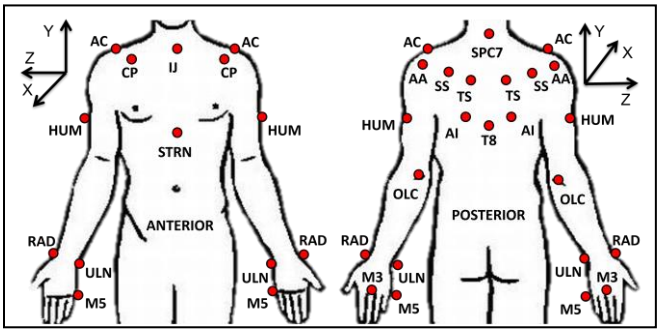

Figure 1. The inverse kinematics model marker locations: xiphoid process (STRN), suprasternal notch (IJ), spinal process C7 (SPC7), spinal process T8 (T8), trigonum spinae (TS), acromial angle (AA), scapular spine (SS; halfway between TS and AA), inferior angle (IA), acromion (AC),coracoid process (CP), lateral aspect of humerus (HUM; technical location), olecranon (OLC), ulnar (ULN) and radial styloids (RAD), and third (M3) & fifth (M5) metacarpals.

C. Inverse Kinematics Model and Rotation Sequences

Our inverse kinematics model with a modified thorax segment was used [9]. Segment coordinate systems for the thorax and the humerus segments are defined using ISB recommendations, Table 1 [3]. The elbow joint center was located anterior of the OLC by an offset equal to the measured elbow width [10]. The location of the glenohumeral (GH) joint center was calculated using updated regression equations developed by Meskers et al., which use the positions of the AC, CP, AA, TS, and IA scapular markers [11]. Due to the subcutaneous motion of the scapula, the TS and IA markers were not tracked dynamically, but recalculated based on the positions of the other scapular markers, following a method developed by Senk and Cheze [6, 9, 12, 13].

TABLE I. COORDINATE SYSTEM DEFINITIONS

Segment	Axis	Definition
Thorax	Superior	Vector connecting midpoint of STRN and T8 to the midpoint of IJ and SPC7
	Lateral	Vector perpendicular to plane STRN, T8, IJ, and SPC7
	Anterior	Cross product of superior & lateral axes
Humerus (ISB option 2)	Superior	Vector connecting elbow joint center to GH joint center
	Lateral	Vector perpendicular to plane elbow joint center, GH joint center, and ULN
	Anterior	Cross product of superior & lateral axes

Coordinate systems followed ISB recommendations with the X axis pointing anteriorly, the Y axis pointing superiorly and Z axis pointing laterally to the participant's right side [3]. For each static position the 3D joint angles of the humerus segment relative to the thorax segment were calculated using seven rotation sequences. Rotations around X-, Y-, and Z- axes representing the coronal, transverse and sagittal planes, respectively (1 – 3) were combined in all possible orders to create the six Cardan rotation matrices (ZXY, ZYX, YXZ, YZX, XYZ, XZY) (4).

$$[R_X(\beta)] = \begin{bmatrix} 1 & 0 & 0 \\ 0 & \cos\beta & -\sin\beta \\ 0 & \sin\beta & \cos\beta \end{bmatrix} \quad (1)$$

$$[R_Y(\gamma)] = \begin{bmatrix} \cos\gamma & 0 & \sin\gamma \\ 0 & 1 & 0 \\ -\sin\gamma & 0 & \cos\gamma \end{bmatrix} \quad (2)$$

$$[R_Z(\alpha)] = \begin{bmatrix} \cos\alpha & -\sin\alpha & 0 \\ \sin\alpha & \cos\alpha & 0 \\ 0 & 0 & 1 \end{bmatrix} \quad (3)$$

$$[R_{TH}] = [R_Z(\alpha)][R_X(\beta)][R_Y(\gamma)], [R_Z(\alpha)][R_Y(\gamma)][R_X(\beta)],$$
$$[R_Y(\gamma)][R_X(\beta)][R_Z(\alpha)], [R_Y(\gamma)][R_Z(\alpha)][R_X(\beta)],$$
$$[R_X(\beta)][R_Y(\gamma)][R_Z(\alpha)], [R_X(\beta)][R_Z(\alpha)][R_Y(\gamma)] \quad (4)$$

For the YXY Euler sequence [3], rotations around the thorax Y-axis, and humerus X- and Y- axes, representing the plane of elevation, elevation angle, and axial rotation (5 – 7) were used to create the rotation sequence (8).

$$[R_{YThorax}(\gamma_T)] = \begin{bmatrix} \cos\gamma_T & 0 & \sin\gamma_T \\ 0 & 1 & 0 \\ -\sin\gamma_T & 0 & \cos\gamma_T \end{bmatrix} \quad (5)$$

$$[R_X(\beta)] = \begin{bmatrix} 1 & 0 & 0 \\ 0 & \cos\beta & -\sin\beta \\ 0 & \sin\beta & \cos\beta \end{bmatrix} \quad (6)$$

$$[R_{YHum}(\gamma_H)] = \begin{bmatrix} \cos\gamma_H & 0 & \sin\gamma_H \\ 0 & 1 & 0 \\ -\sin\gamma_H & 0 & \cos\gamma_H \end{bmatrix} \quad (7)$$

$$[R_{TH}] = [R_{YThorax}(\gamma_T)][R_X(\beta)][R_{YHum}(\gamma_H)] \quad (8)$$

D. Data Analysis

Three-dimensional positions of the markers were reconstructed in Vicon Nexus software and filtered using a Woltring filter (MSE = 20). The upper extremity inverse kinematics model calculated the 3D thoracohumeral (TH) joint motions for the left and right arms of each trial using each of the seven rotation sequences. Data from both arms were included for each subject (eight total measurements) to calculate a group average and standard deviation, which were compared to the goniometric measure. Errors within +/- 5 deg were considered good, and errors within +/- 10 deg were considered acceptable. Data were also reviewed to determine incidence of gimbal lock. For each static posture, a trial that resulted in this mathematically indeterminant calculation (division by 0) was counted as gimbal lock.

III. RESULTS

A. Incidence of Gimbal Lock

Incidence of gimbal lock, based on number of trials out of eight total (two right, two left, per participant) is presented in Table 2.

TABLE II. INCIDENCE OF GIMBAL LOCK

Posture	Rotation Sequence						
	YXY	ZXY	ZYX	YXZ	YZX	XYZ	XZY
1: EP 0°, EA 0°	0	0	2	0	0	0	0
2: EP 0°, EA 45°	0	2	4	0	0	8	4
3: EP 0°, EA 90°	0	8	4	0	0	4	4
4: EP 0°, EA 120°	0	8	4	0	4	3	4
5: EP 90°, EA 45°	0	0	0	0	0	0	0
6: EP 90°, EA 90°	0	0	0	0	0	0	0
7: EP 90°, EA 120°	0	0	0	0	5	0	4
8: EP -90°, EA 30°	0	0	0	0	0	0	0
9: EP 0°, EA 0°, Int 30°	0	0	0	0	0	0	0
10: EP 0°, EA 0°, Ext 30°	0	0	0	0	0	0	0
11: EP 0°, EA 90°, Int 30°	0	8	4	0	4	4	4
12: EP 0°, EA 90°, Int 90° -only 6 trials	0	6	3	0	2	3	3

B. Thoracohumeral Joint Angles

Group average thoracohumeral (TH) joint angles, along with the goniometric value are presented in Tables 3-5.

TABLE III. GONIOMETRIC AND GROUP AVERAGE (+/-1 STDEV) CALCULATED TH JOINT ANGLES WITH EACH ROTATION SEQUENCE FOR CORONAL PLANE POSTURES (EP = ELEVATION PLANE ANGLE; EA = ELEVATION ANGLE). GREEN INDICATES ERROR WITHIN ± 5° OF GONIOMETER, YELLOW WITHIN ±10°.

	Posture 1 (arms at side)		Posture 2 (abduction)		Posture 3		Posture 4	
Goniometer	**EP = 0°**	**EA = 0°**	**EP = 0°**	**EA = -45°**	**EP = 0°**	**EA = -90°**	**EP = 0°**	**EA = -120°**
YXY	-67.2 (41.7)	-8.8 (3.1)	-7.8 (7.1)	-37.5 (2.3)	-0.1 (3.4)	-73.3 (2.3)	8.0 (3.8)	-100.7 (2.4)
ZXY	-11.6 (7.7)	-1.4 (8.4)	-11.5 (7.7)	-70.6 (3.5)	-	-	-	-
ZYX	1.4 (15.2)	1.3 (43.2)	118.4 (17.4)	-96.8 (3.6)	115.1 (2.9)	-90.7 (0.4)	113.7 (3.2)	-84.7 (0.8)
YXZ	0.5 (2.5)	-3.1 (0.8)	19.6 (3.6)	0.7 (2.9)	55.7 (5.1)	10.0 (4.5)	115.1 (6.0)	11.1 (3.0)
YZX	0.6 (2.4)	-3.1 (0.8)	17.2 (3.2)	0.8 (3.0)	37.6 (8.6)	17.4 (7.4)	-	-
XYZ	-43.3 (29.1)	-19.6 (11.3)	-	-	160.7 (8.5)	101.7 (4.9)	121.9 (3.8)	34.9 (5.6)
XZY	-11.4 (7.2)	-1.3 (8.4)	-1.9 (1.2)	-52.5 (1.9)	3.1 (1.4)	-80.2 (2.7)	14.0 (0.8)	-97.2 (0.4)

TABLE IV. GONIOMETRIC AND GROUP AVERAGE (+/-1 STDEV) CALCULATED TH JOINT ANGLES WITH EACH ROTATION SEQUENCE FOR SAGITTAL PLANE POSTURES (EP = ELEVATION PLANE ANGLE; EA = ELEVATION ANGLE). GREEN INDICATES ERROR WITHIN ± 5° OF GONIOMETER, YELLOW WITHIN ±10°.

	Posture 5 (extension)		Posture 6 (flexion)		Posture 7		Posture 8	
Goniometer	**EP: -90° (YXY) 0° (Cardan)**	**EA = -30°**	**EP: 90° (YXY) 0° (Cardan)**	**EA: -45° (YXY) 45° (Cardan)**	**EP: 90° (YXY) 0° (Cardan)**	**EA: -90° (YXY) 90° (Cardan)**	**EP: 90° (YXY) 0° (Cardan)**	**EA: -120° (YXY) 120° (Cardan)**
YXY	-86.6 (3.7)	-33.1 (2.4)	90.4 (8.8)	-25.1 (3.4)	87.3 (3.6)	-63.7 (3.5)	79.2 (4.5)	-93.0 (2.9)
ZXY	-1.8 (3.1)	-46.9 (3.4)	0.2 (6.4)	38.7 (2.9)	-3.9 (5.4)	74.3 (1.4)	-18.3 (6.8)	92.3 (1.7)
ZYX	-4.4 (14.9)	-20.5 (4.8)	4.9 (16.5)	14.9 (4.8)	-6.1 (10.1)	51.2 (6.3)	-28.9 (5.7)	90.0 (6.8)
YXZ	-10.1 (2.2)	-6.1 (4.5)	3.7 (1.9)	7.6 (4.5)	5.8 (4.3)	31.6 (10.9)	-19.1 (5.1)	103.9 (10.3)
YZX	-10.1 (2.1)	-5.5 (3.7)	3.7 (1.9)	7.2 (4.2)	6.5 (4.6)	22.0 (8.0)	-100.6 (27.1)	63.3 (16.1)
XYZ	-31.9 (17.6)	-73.2 (10.6)	9.6 (8.1)	60.2 (9.0)	7.3 (5.8)	82.1 (2.6)	-12.3 (3.7)	89.6 (1.5)
XZY	-2.1 (3.7)	-44.2 (3.1)	0.1 (7.1)	37.5 (3.6)	-9.5 (12.5)	67.9 (2.5)	-104.9 (12.5)	76.0 (7.1)

TABLE V. GONIOMETRIC AND GROUP AVERAGE (+/-1 STDEV) CALCULATED TH JOINT ANGLES WITH EACH ROTATION SEQUENCE FOR AXIAL ROTATION POSTURES (EP = ELEVATION PLANE ANGLE; EA = ELEVATION ANGLE). GREEN INDICATES ERROR WITHIN ± 5° OF GONIOMETER, YELLOW WITHIN ±10°.

	Posture 9 (adduct. internal rot.)			Posture 10 (add. external rot.)			Posture 11 (abduct. int. rot.)			Posture 12 (abd. int. rot.)		
Goniometer	**EP = 0°**	**EA = 0°**	**Axial = 30°**	**EP = 0°**	**EA = 0°**	**Axial: -30°**	**EP = 0°**	**EA = -90°**	**Axial: -60°**	**EP = 0°**	**EA = -90°**	**Axial = 0°**
YXY	-54.8 (19.0)	-10.7 (0.7)	79.1 (17.3)	-79.6 (38.6)	-8.0 (2.1)	46.5 (38.1)	2.2 (4.4)	-75.8 (1.4)	-57.3 (2.1)	-0.6 (3.2)	-78.9 (3.3)	-1.3 (4.7)
ZXY	-13.8 (4.0)	-8.9 (4.7)	22.1 (4.4)	-11.1 (6.1)	-0.2 (6.5)	-35.8 (4.3)	-	-	-	-	-	-
ZYX	-6.6 (0.8)	-6.1 (3.8)	26.1 (2.8)	-3.6 (3.5)	-0.4 (5.1)	-40.4 (5.1)	42.1 (3.2)	-77.9 (3.9)	-9.7 (1.7)	2.5 (2.3)	-78.1 (3.2)	0.8 (3.0)
YXZ	-10.0 (0.8)	-2.0 (3.2)	22.7 (4.6)	-5.0 (4.8)	-4.3 (2.2)	-35.7 (4.4)	73.8 (1.8)	-31.1 (2.1)	-79.0 (5.0)	12.7 (26.1)	-77.7 (2.6)	-11.4 (28.7)

YZX	-10.0 (1.1)	-2.0 (3.2)	22.3 (4.3)	-5.0 (4.6)	-4.3 (2.2)	-36.0 (4.4)	43.4 (2.4)	-64.0 (1.6)	-22.2 (2.9)	-0.2 (4.8)	-79.9 (3.8)	-2.2 (3.7)
XYZ	-9.0 (1.8)	-1.5 (2.2)	27.1 (4.7)	-8.2 (4.2)	-3.3 (1.8)	-39.3 (4.6)	-2.1 (3.3)	-69.9 (7.5)	-58.8 (1.1)	-2.5 (3.0)	-73.4 (7.8)	1.0 (7.8)
XZY	-13.7 (4.1)	-8.9 (4.6)	22.9 (4.6)	-11.2 (5.7)	-0.2 (6.5)	-35.9 (4.5)	6.6 (4.7)	-81.4 (0.6)	-55.7 (1.3)	1.6 (2.7)	-82.7 (1.4)	-3.3 (4.0)

IV. Discussion

We successfully modeled 3D thoracohumeral joint motion using seven rotation sequences and compared the resulting joint angles to goniometric values as ground truth. Incidences of gimbal lock and joint angle errors were examined to assess the effects of each rotation sequence on thoracohumeral joint angles.

The only sequences to experience no gimbal lock across all 12 postures were YXY and YXZ. The ZXY sequence experienced gimbal lock for all trials of four postures, specifically those with high degrees of abduction in the coronal plane, and both internal rotation postures with the arm abducted. For five of the 12 postures, gimbal lock was not present with any sequences. These five postures were: 30° of extension and 45° and 90° of flexion in the sagittal plane, and 30° of internal and external rotation with the arm adducted. There were multiple postures during which gimbal lock occurred for only half of the trials. This typically presented for the entirety of one of the two participants, however not always the same participant. The reasoning for which requires further investigation but is hypothesized to be due to anatomical differences.

The computed joint angles were compared with the goniometric measurement to determine joint angle error. We selected ±10° as acceptable error and ±5° as good error. Depending on the clinical application, such as for surgical decision making, joint angle errors may need to be within the smaller range. For the four coronal plane postures (Table 3), the XZY rotation sequence had the lowest errors for the most postures, whereas the XYZ sequence had unacceptable errors across all postures, closely followed by ZXY and ZYX. All rotation sequences had unacceptable errors at 120° of abduction or flexion (Tables 3-4). This is a well-known limitation and ongoing challenge for modeling the shoulder at and above 120° of elevation. For the other three sagittal plane postures (Table 4), the sequence(s) with the lowest errors was dependent on the posture: YXY and ZYX at 30° extension, ZXY and XZY at 45° flexion, and XYZ at 90° flexion. For the four axial rotations (Table 5), the XYZ sequence had the best errors for the most postures, followed by the XZY (best in abducted postures) and YZX (best in adducted postures) sequences. ZXY and YXZ only performed well when the arm was in the adducted postures, and YXY only performed well in the abducted postures. While generally low, especially for measurements with good or acceptable error, most of the variability that occurred was between participants, with only a few instances of within participant between arm variability. These are likely a result of anatomical differences and bilateral asymmetries, but warranty further consideration.

V. Conclusion

These results support the hypothesis that the rotation sequence used for modeling should be chosen based on the posture of the TH joint during the task of interest. Current work is underway with more participants exploring the effects of rotation sequence as the arm moves through a range of complex motions. We anticipate more definitive recommendations on rotation sequence selection will be clear through the combined analyses of the static postures reported here and dynamic tasks. This work will aid in decision making for selecting the appropriate rotation sequence for specific movement tasks and postures and help elucidate the effects that a biomechanical modeling sequence has on the clinical implications of joint angle interpretation.

References

[1] A. M. Valevicius, P. Y. Jun, J. S. Hebert, and A. H. Vette, "Use of optical motion capture for the analysis of normative upper body kinematics during functional upper limb tasks: A systematic review," *J Electromyogr Kinesiol,* vol. 40, pp. 1-15, 2018.

[2] A. Bonnefoy-Mazure, J. Slawinski, A. Riquet, J.-M. Lévèque, C. Miller, and L. Cheze, "Rotation sequence is an important factor in shoulder kinematics. Application to the elite players' flat serves," *J Biomech,* vol. 43, no. 10, pp. 2022-2025, 2010.

[3] G. Wu *et al.*, "ISB recommendation on definitions of joint coordinate systems of various joints for the reporting of human joint motion—Part II: shoulder, elbow, wrist and hand," *J Biomech,* vol. 38, no. 5, pp. 981-992, 2005.

[4] P. J. Rundquist and P. M. Ludewig, "Correlation of 3-dimensional shoulder kinematics to function in subjects with idiopathic loss of shoulder range of motion," *Physical therapy,* vol. 85, no. 7, pp. 636-647, 2005.

[5] P. J. Rundquist, C. Obrecht, and L. Woodruff, "Three-dimensional shoulder kinematics to complete activities of daily living," *Am J Phys Med Rehabil,* vol. 88, no. 8, pp. 623-9, Aug 2009, doi: 10.1097/PHM.0b013e3181ae0733.

[6] M. Šenk and L. Cheze, "Rotation sequence as an important factor in shoulder kinematics," *Clinical biomechanics,* vol. 21, pp. S3-S8, 2006.

[7] A. R. Karduna, P. W. McClure, and L. A. Michener, "Scapular kinematics: effects of altering the Euler angle sequence of rotations," *J Biomech,* vol. 33, no. 9, pp. 1063-1068, 2000.

[8] G. Rab, K. Petuskey, and A. Bagley, "A method for determination of upper extremity kinematics," *Gait & posture,* vol. 15, no. 2, pp. 113-119, 2002.

[9] A. J. Schnorenberg, B. A. Slavens, M. Wang, L. C. Vogel, P. A. Smith, and G. F. Harris, "Biomechanical model for evaluation of pediatric upper extremity joint dynamics during wheelchair mobility," *J Biomech,* vol. 47, no. 1, pp. 269-276, 2014.

[10] B. Hingtgen, J. R. McGuire, M. Wang, and G. F. Harris, "An upper extremity kinematic model for evaluation of hemiparetic stroke," *J Biomech,* vol. 39, no. 4, pp. 681-688, 2006.

[11] C. Meskers, F. C. Van der Helm, L. Rozendaal, and P. Rozing, "In vivo estimation of the glenohumeral joint rotation center from scapular bony landmarks by linear regression," *J Biomech,* vol. 31, no. 1, pp. 93-96, 1997.

[12] M. Šenk and L. Cheze, "A new method for motion capture of the scapula using an optoelectronic tracking device: a feasibility study," *Comput Methods Biomech Biomed Engin,* vol. 13, no. 3, pp. 397-401, 2010.

[13] A. J. Schnorenberg, M. E. French, J. M. Riebe, S. I. Grindel, and B. A. Slavens, "Shoulder complex kinematics pre-and post-rotator cuff repair," *J Electromyogr Kinesiol,* p. 102331, 2019.